ACS APPLIED ENERGY MATERIALS

Letter

Cite This: ACS Appl. Energy Mater. 2019, 2, 3009−3012

www.acsaem.org

Electrodeposition of the NaK Alloy with a Liquid Organic Electrolyte

Rodrigo Rodriguez,[†] Ruth A. Edison,[†] Adam Heller,[†,∥] and C. Buddie Mullins*[,†,‡,§,∥]

[†]McKetta Department of Chemical Engineering, The University of Texas at Austin, Austin, Texas 78712-1589, United States

[‡]Texas Materials Institute, The University of Texas at Austin, Austin, Texas 78712-1591, United States

[§]Department of Chemistry, The University of Texas at Austin, Austin, Texas 78712-1224, United States

[∥]Center for Electrochemistry, The University of Texas at Austin, Austin, Texas 78712-0165, United States

Supporting Information

ABSTRACT: Sodium−potassium alloys have recently been proposed as anode materials for liquid metal batteries because they can form a liquid phase at room temperature for a wide range of compositions. In this work, the electrodeposition morphology of this NaK alloy is revealed through in situ optical imaging. We report that the NaK alloy deposits dendritically akin to solid sodium anodes in liquid organic electrolytes. However, when sodium is deposited on a potassium-rich alloy, dendrite formation is greatly mitigated but not prevented.

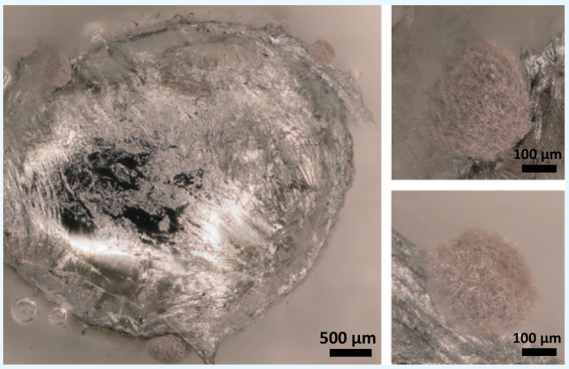

KEYWORDS: *sodium, potassium, alloy, dendrite, battery, FEC*

Liquid metal batteries (LMBs) offer a wide variety of benefits over traditional lithium-ion batteries (LIBs). Since LMBs do not utilize slurry cast films, which can crack, delaminate, and deteriorate as the battery is cycled, the operating lifetimes of LMBs are much longer than conventional secondary batteries.[1] The liquid−liquid interfaces present in LMBs also endow these batteries with transport kinetics that are vastly superior to LIBs, enabling ultrafast charging rates.[2,3] Additionally, the LMB's electrode and electrolyte components naturally phase separate, which obviates the need for a separator and simplifies the cell design.[3] The earth abundant materials utilized in these liquid batteries further reduce their costs as well.[1,3,4] Though liquid metal batteries have low theoretical energy densities, their cheap materials and separator free cell design make LMBs a potential candidate for large-scale, stationary energy storage.[2]

Sodium metal anodes cycled in organic electrolytes electrodeposit dendritically. This deposition behavior can cause dangerous internal shorting and results in low cycling efficiencies. LMBs can circumvent this problem by maintaining a liquid phase at the anode so that the formation of solid dendrites is prevented.[5] However, one of the major drawbacks of LMBs is the high operating temperature required to retain the battery components above their melting points.[6,7] Maintaining high temperatures is costly and can also accelerate long-term cell corrosion caused by the chemical attack of the electrodes toward the cell lining.[2] Recently, Goodenough and co-workers reported that the liquid sodium−potassium (NaK) alloy could be cycled with a liquid organic electrolyte at room temperature.[4] Utilizing either a metal foam or carbon fiber host to house the NaK alloy, they were able to cycle the electrode in an electrolyte of 1 M $NaClO_4$ in propylene carbonate/fluoroethylene carbonate (FEC).[4,8] Symmetrical cells of the alloy revealed improved cycling stability compared to the control, symmetrical Na cells. Additionally, a sodiated $Na_2MnFe(CN)_6$ cathode was shown to cycle with the NaK alloy.[9]

The NaK alloy remains liquid at room temperature from 29 to 86 at. % K; outside of this range a liquid and a solid solution exist simultaneously. If sodium is chosen as the electrochemically active metal, an alloy with the highest potassium content that retains the liquid phase (86% K at room temperature) would allow the maximum amount of sodium uptake before returning to a liquid/solid phase at the equilibrium line. However, a concentration front enriched with sodium may form at the alloy's surface if sodium is the only electrodeposited metal. If interdiffusion of sodium and potassium is slower than the flux of sodium entering the alloy's surface, formation of a solid solution could be a possibility and dendrite formation may reemerge.

In this letter, we examine the electrodeposition of sodium on a NaK alloy housed inside nickel foam. A 1 M $NaPF_6$ in FEC/diethylene carbonate (DEC) (1:1 by volume) electrolyte was used for all depositions. In order to conduct in situ imaging of the electrodeposition of sodium into the NaK alloy, a home-

Received: February 13, 2019
Accepted: April 19, 2019
Published: April 19, 2019

DOI: 10.1021/acsaem.9b00311
ACS Appl. Energy Mater. 2019, 2, 3009−3012

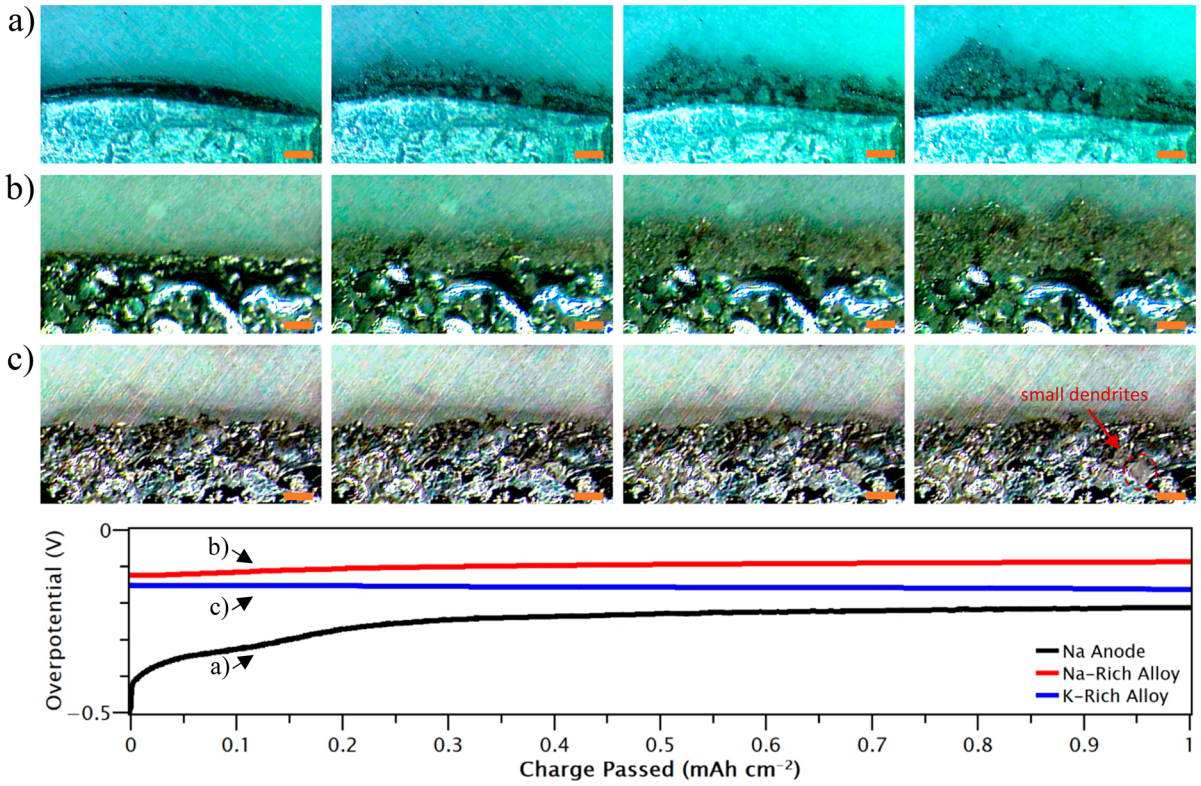

Figure 1. Sequential imaging of (a) sodium, (b) Na−K alloy (67 at. % Na), and (c) Na−K alloy (17 at. % Na) as 1 mAh cm^{-2} of charge is passed at 2 mA cm^{-2}. The corresponding overpotential curves for all three electrodes are shown below. The scale bars are 150 μm.

built visualization cell was utilized in conjunction with a USB microscope. In situ optical imaging revealed that dendritic structures can electrodeposit on the surface of the NaK liquid alloy at both slow (0.5 mA cm^{-2}) and fast (2.0 mA cm^{-2}) rates. However, the formation of dendrites could be greatly mitigated by depositing the sodium into a potassium-rich alloy at fast charge rates.

Figure 1 shows sequential imaging of sodium electrodepositing on (a) sodium, (b) Na-rich NaK alloy, and (c) K-rich NaK alloy electrodes after passing 0, 0.33, 0.66, and 1 mAh cm^{-2} of charge at a rate of 2 mA cm^{-2}. In the visualization cell, the electrodes were physically held 1 mm apart from each other without a separator. Thus, no compressive forces were acting on the electrode surfaces during all electrodepositions. In order to establish adequate electrical contact with the liquid electrodes, a nickel foam host was utilized to house the alloys (Figure S2). These liquid alloys were inserted into the nickel foam using vacuum infiltration as the high surface tension of the alloy does not allow the liquid to penetrate the foam readily.[8] All the depositions in the visualization cell utilized a solid sodium counter/reference electrode without the nickel foam host. A 1 M $NaPF_6$ in FEC/DEC (50 vol. % FEC) electrolyte was chosen over the 1 M $NaClO_4$ in propylene carbonate/FEC (10 vol. % FEC) electrolyte in this study in order to improve solvent compatibility with the alkali metals.[10,11] Our group has shown that the high content of FEC in the 1 M $NaPF_6$ in FEC/DEC electrolyte can create a fluorine-rich, passivating solid electrolyte interphase that greatly mitigates gas formation.[10]

The concentrations of the alloys were chosen by drawing a tie line through the NaK phase diagram at 20 °C and selecting the atomic percentages of the elements at the liquid/solid equilibrium line (see Supporting Information Figure S1). This ensured that the Na-rich (33 at. % K) and K-rich (82 at. % K) alloys had the highest concentration of the desired element while maintaining the liquid phase at room temperature (~25 °C). These compositions, Na- or K-rich alloys, were chosen to study the electrodeposition behavior of the alloy at the two extremes of the liquid phase; alloy concentrations between the selected Na- and K-rich alloys should exhibit similar behavior. The formation of a sodium-enriched surface during electrodeposition should be retarded by the K-rich alloy since the magnitude of a concentration gradient in a solution impacts the rate at which mass transport occurs. Thus, the formation of a sufficiently rich sodium surface capable of nucleating a sodium dendrite should occur more readily in a Na-rich alloy than in a K-rich alloy.

For depositions of sodium onto a sodium electrode (Figure 1a), the formation of dendritic structures is observed. The overpotential starts out high but plateaus around 200 mV after sodium deposits have begun to nucleate and grow. For both liquid alloy depositions, no such steep overpotential drop is observed. The overpotential is a product of many factors required for electron transfer from the electrode to the solvated ion species. Since the electrolyte used in all of the depositions is the same, differences in the overpotential across all trials should be a product of surface conditions such as native oxide layers, SEI, and phase.[12,13] Since the alloy contains two species of alkali metal that are highly reactive toward the electrolyte, their SEI layer must be an amalgamation of both potassium and sodium based decomposition products. Perhaps this SEI has a lower impedance than the SEI formed on a sodium electrode. A study of the SEI formed with the bimetallic NaK alloy would be worth exploring but is beyond the scope of this letter. Additionally, the Cui group has shown that some alloys

DOI: 10.1021/acsaem.9b00311
ACS Appl. Energy Mater. 2019, 2, 3009−3012

of lithium can reduce the nucleation overpotential to initialize lithium electrodeposition.[14] Something similar could be occurring here as well. Finally, the vacuum filtration technique used to create the nickel foam/liquid alloy electrodes also results in pristine surfaces. Thus, a high polarization energy may not be required to nucleate the liquid alloys since only a nascent oxide layer is present on the NaK surface.

Despite recent reports, we found that the NaK liquid alloy forms solid electrodeposits in liquid organic electrolytes (Figure 1b). However, their formation was found to be greatly mitigated when the liquid alloy's Na content was kept low (Figure 1c). This reduction in dendrite formation is also reflected in the corresponding voltage profile. For the liquid alloy that has high Na content (Figure 1b), the overpotential does decrease as dendrites begin to form due to the increased surface area. This is not seen in the alloy with low Na content in which dendrite formation is mitigated. However, when the charge passed in the K-rich alloy was increased from 1 to 3 mAh cm^{-2}, the resurgence of larger dendritic structures was observed (Figure 2).

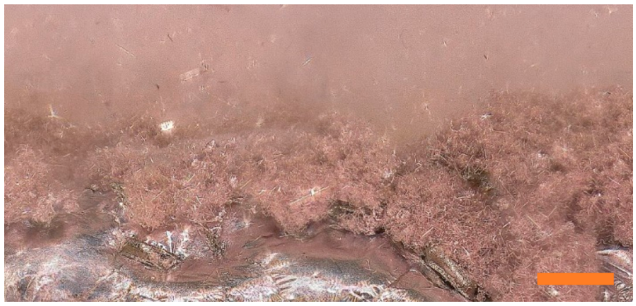

Figure 2. High-resolution imaging of the K-rich NaK alloy after 3 mAh cm^{-2} of charge has been passed with a 2 mA cm^{-2} charge rate. Scale bar is 250 μm.

We attribute dendrite formation to the compositional inhomogeneity of the electrodeposited alloy, which is liquid only for a defined range of Na/K ratios but is solid when the deposit is either Na- or K-rich. As sodium ions are reduced at the surface and enter the liquid alloy, the composition shifts from the bulk concentration to a more sodium-enriched one. If this occurs, part of the liquid alloy will be shifted from the liquid phase to the solid sodium phase where potassium is dissolved in a solid solution. This phenomenon is illustrated in Figure 3. Thus, the formation of dendrites on this liquid alloy could be attributed to its bimetallic composition since other single element liquid alloys do not form dendritic depositions. If a cathode material could desodiate and depotassiate at a ratio equal to a NaK liquid alloy, it is possible that dendrite formation could be eliminated. Additionally, such a cathode would greatly increase the energy density of a NaK liquid metal battery since both of the bimetallic constituents would be participating in the electrochemistry.

If the slow diffusion of sodium into the bulk of the alloy is the reason for dendrite formation, then lowering the charge rate should help mitigate their formation since the flux of sodium entering the alloy would be lower. Figure 4 shows that dropping the charging current 4-fold to 0.5 mA cm^{-2} actually exacerbates the formation of dendrites on the K-rich alloy. Comparing the overpotential curves in Figure 4, the appearance of a nucleation overpotential peak is observed in the slow rate curve (black) and not in the fast rate curve (red). The nucleation overpotential peak is not a function of the charge rate.[15] Thus, at a fast rate (2.0 mA cm^{-2}), the overpotential required to deposit sodium is always higher than the nucleation overpotential. This ensures a high nuclei density which mitigates the formation of larger dendritic structures observed at slower charge rates (Figure 4). Therefore, it appears that both a fast charge rate and low bulk sodium content are required for dendrite mitigation. It is also possible that the dendrites could dissolve back into the alloy given enough time. However, we saw no noticeable change in dendrite heights after letting deposits sit for 4 h. The persistence of these solid sodium dendrites is not caused by passing sufficient charge to affect the bulk concentration since the total electrode mass is much larger than the mass of the deposited sodium. It is possible that the time required for the alloy and sodium dendrites to return to a bulk concentration is much longer than 4 h or perhaps a similar effect to "dead-lithium" formation may be occurring here as well.

In conclusion, we have shown for the first time the electrodeposition behavior of the liquid NaK alloy in a liquid organic electrolyte. The appearance of solid dendrites on the alloy's liquid surface is attributed to its bimetallic composition as dendrite formation does not occur on pure liquid sodium anodes. The potassium bulk content was found to greatly decrease the formation of dendrites. This was attributed to the faster rate of sodium dissolution in the K-rich alloy, which slowed the formation of a Na-enriched surface that could nucleate solid sodium. It was also shown that, akin to solid alkali metals, the charge rate reduced the formation of large dendritic structures by increasing the nuclei density on the NaK surface. The appeal of the NaK alloy was the room temperature liquid phase which was thought to cycle without forming dendrites and reduce the operating temperatures of a liquid metal battery. Though we have shown this is not the case, there may still be ways of achieving dendrite free

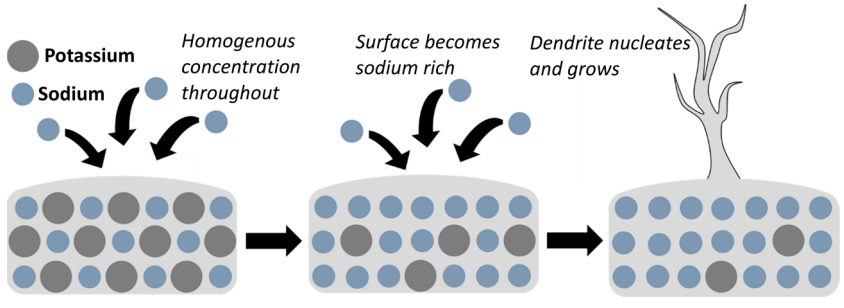

Figure 3. Nucleation of a solid sodium dendrite on a liquid alloy.

DOI: 10.1021/acsaem.9b00311
ACS Appl. Energy Mater. 2019, 2, 3009−3012

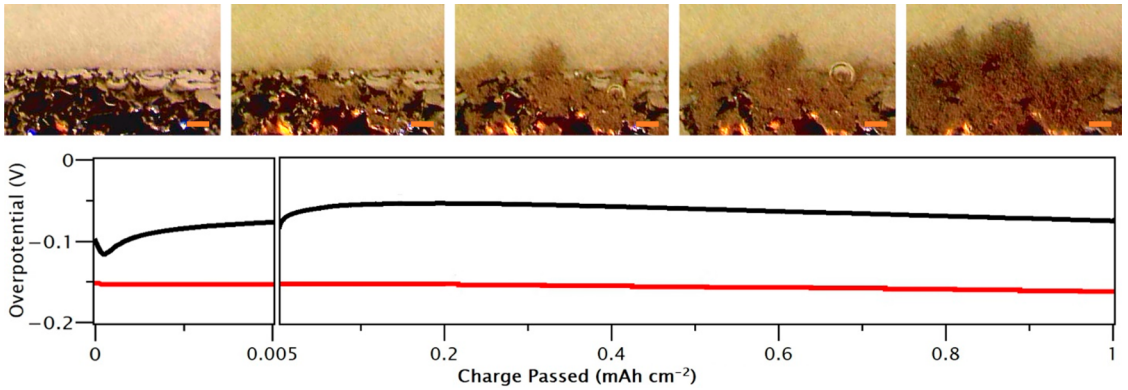

Figure 4. Sequential imaging of K-rich alloy (17 at. % Na) as 1 mAh cm^{-2} of charge is passed at 0.5 mA cm^{-2}. The black curve is the overpotential curve for the imaged deposition (slow rate), and the red curve is for the fast rate deposition of the same alloy composition from Figure 1. Scale bars are 500 μm.

depositions as has been done with lithium anodes through electrolyte additives[16] or modifying the NaK liquid surface.[17]

■ ASSOCIATED CONTENT

Supporting Information

The Supporting Information is available free of charge on the ACS Publications website at DOI: 10.1021/acsaem.9b00311.

Experimental procedures (PDF)

■ AUTHOR INFORMATION

Corresponding Author

*E-mail: mullins@che.utexas.edu.

ORCID

Adam Heller: 0000-0003-0181-1246

C. Buddie Mullins: 0000-0003-1030-4801

Notes

The authors declare no competing financial interest.

■ ACKNOWLEDGMENTS

We acknowledge the generous support of the Welch Foundation (via Grant Nos. F-1131 (AH) and F-1436 (CBM)) as well as that of the National Science Foundation through Grant No. CBET-1603491. R.R. acknowledges the Peter Buenz fellowship through the Cockrell School of Engineering for financial support. We thank Celgard Corp. for their provision of separators and Solvay Fluor for their donation of fluoroethylene carbonate. We also thank Dr. Krishnaswamy Ravi-Chandar for use of his Keyence VHX-5000 digital microscope.

■ REFERENCES

(1) Ashour, R. F.; Kelley, D. H.; Salas, A.; Starace, M.; Weber, N.; Weier, T. Competing Forces in Liquid Metal Electrodes and Batteries. *J. Power Sources* **2018**, *378*, 301−310.

(2) Kim, H.; Boysen, D. A.; Newhouse, J. M.; Spatocco, B. L.; Chung, B.; Burke, P. J.; Bradwell, D. J.; Jiang, K.; Tomaszowska, A. A.; Wang, K.; Wei, W.; Ortiz, L. A.; Barriga, S. A.; Poizeau, S. M.; Sadoway, D. R. Liquid Metal Batteries: Past, Present, and Future. *Chem. Rev.* **2013**, *113*, 2075−2099.

(3) Bradwell, D. J.; Kim, H.; Sirk, A. H. C.; Sadoway, D. R. Magnesium−Antimony Liquid Metal Battery for Stationary Energy Storage. *J. Am. Chem. Soc.* **2012**, *134*, 1895−1897.

(4) Xue, L.; Gao, H.; Zhou, W.; Xin, S.; Park, K.; Li, Y.; Goodenough, J. B. Liquid K−Na Alloy Anode Enables Dendrite-Free Potassium Batteries. *Adv. Mater.* **2016**, *28*, 9608−9612.

(5) Ellis, B. L.; Nazar, L. F. Sodium and Sodium-Ion Energy Storage Batteries. *Curr. Opin. Solid State Mater. Sci.* **2012**, *16*, 168−177.

(6) Wang, K.; Jiang, K.; Chung, B.; Ouchi, T.; Burke, P. J.; Boysen, D. A.; Bradwell, D. J.; Kim, H.; Muecke, U.; Sadoway, D. R. Lithium−Antimony−Lead Liquid Metal Battery for Grid-Level Energy Storage. *Nature* **2014**, *514*, 348−350.

(7) Li, H.; Wang, K.; Cheng, S.; Jiang, K. High Performance Liquid Metal Battery with Environmentally Friendly Antimony−Tin Positive Electrode. *ACS Appl. Mater. Interfaces* **2016**, *8*, 12830−12835.

(8) Xue, L.; Zhou, W.; Xin, S.; Gao, H.; Li, Y.; Zhou, A.; Goodenough, J. B. Room-Temperature Liquid Na−K Anode Membranes. *Angew. Chem., Int. Ed.* **2018**, *57*, 14184−14187.

(9) Xue, L.; Gao, H.; Li, Y.; Goodenough, J. B. Cathode Dependence of Liquid-Alloy Na−K Anodes. *J. Am. Chem. Soc.* **2018**, *140*, 3292−3298.

(10) Rodriguez, R.; Loeffler, K. E.; Nathan, S. S.; Sheavly, J. K.; Dolocan, A.; Heller, A.; Mullins, C. B. In Situ Optical Imaging of Sodium Electrodeposition: Effects of Fluoroethylene Carbonate. *ACS Energy Lett.* **2017**, *2*, 2051−2057.

(11) Chen, X.; Shen, X.; Li, B.; Peng, H.-J.; Cheng, X.-B.; Li, B.-Q.; Zhang, X.-Q.; Huang, J.-Q.; Zhang, Q. Ion−Solvent Complexes Promote Gas Evolution from Electrolytes on a Sodium Metal Anode. *Angew. Chem., Int. Ed.* **2018**, *57*, 734−737.

(12) Bieker, G.; Winter, M.; Bieker, P. Electrochemical in Situ Investigations of SEI and Dendrite Formation on the Lithium Metal Anode. *Phys. Chem. Chem. Phys.* **2015**, *17*, 8670−8679.

(13) Wood, K. N.; Kazyak, E.; Chadwick, A. F.; Chen, K.-H.; Zhang, J.-G.; Thornton, K.; Dasgupta, N. P. Dendrites and Pits: Untangling the Complex Behavior of Lithium Metal Anodes through Operando Video Microscopy. *ACS Cent. Sci.* **2016**, *2*, 790−801.

(14) Yan, K.; Lu, Z.; Lee, H.-W.; Xiong, F.; Hsu, P.-C.; Li, Y.; Zhao, J.; Chu, S.; Cui, Y. Selective Deposition and Stable Encapsulation of Lithium through Heterogeneous Seeded Growth. *Nat. Energy* **2016**, *1*, 16010.

(15) Pei, A.; Zheng, G.; Shi, F.; Li, Y.; Cui, Y. Nanoscale Nucleation and Growth of Electrodeposited Lithium Metal. *Nano Lett.* **2017**, *17*, 1132−1139.

(16) Wang, D.; Zhang, W.; Zheng, W.; Cui, X.; Rojo, T.; Zhang, Q. Towards High-Safe Lithium Metal Anodes: Suppressing Lithium Dendrites via Tuning Surface Energy. *Adv. Sci.* **2017**, *4*, 1600168.

(17) Zhang, L.; Xia, X.; Zhong, Y.; Xie, D.; Liu, S.; Wang, X.; Tu, J. Exploring Self-Healing Liquid Na−K Alloy for Dendrite-Free Electrochemical Energy Storage. *Adv. Mater.* **2018**, *30*, 1804011.

DOI: 10.1021/acsaem.9b00311
ACS Appl. Energy Mater. 2019, 2, 3009−3012